

Analysis of dispersion characteristics of solid-core PCFs with different types of lattice in the claddings, infiltrated with ethanol

Bao Tran Le Tran¹, Thuy Nguyen Thi¹, Ngoc Vo Thi Minh², Trung Le Canh³, Minh Le Van⁴, Van Cao Long⁵, Khoa Dinh Xuan³, Lanh Chu Van^{*3}

¹Hue University of Education, Hue University, 34 Le Loi Street - Hue City, Viet Nam

²Huynh Thuc Khang High School, La Grai district, Gia Lai Province, Viet Nam

³Department of Physics, Vinh University, 182 Le Duan, Vinh City, Viet Nam

⁴School of Engineering and Technology, Vinh University, 182 Le Duan, Vinh city, Vietnam

⁵Institute of Physics, University of Zielona Góra, Prof. Szafrana 4a, 65-516 Zielona Góra, Poland;

Received October 25, 2020; accepted December 18, 2020; published December 31, 2020

Abstract—In this paper, we propose three solid-core photonic crystal fibers based on silica, with hexagonal, circular and square lattices as a cladding, composed of 8 rings of air-holes surrounding the core, infiltrated with ethanol. Using commercial software, we simulated light propagation in these structures. The size of air-holes was from 1 μm to 4 μm . We have shown that the fibers with hexagonal lattices are optimal for supercontinuum generation since their dispersion characteristics are flat and the smallest.

Photonic crystal fibers (PCF) were invented by Knight and his colleagues in 1996 [1]. Since then, they have allowed for a breakthrough in fiber optic technology due to their unique properties and possibilities of application not achievable with conventional optical fibers.

The properties of PCFs can be tuned with a properly designed internal structure. Geometrical parameters related to the structure include the shape and size of lattice in the cladding, the shape and size of air-holes, and the lattice constant [2]. In addition, for solid-core and hollow-core PCFs, the transmission mechanism is different [3, 4]. The most important optical parameters of PCFs include an effective refractive index, effective mode area, dispersion, and attenuation [5, 6].

The choice of the type of lattice constituting the fiber photonic cladding is determined by the planned application. Hexagonal lattices were used, e.g., for efficient femtosecond laser grating inscription [7], dispersion management [8], confinement loss control [9], and broadband infrared supercontinuum generation [10]. Circular lattices were presented to achieve effective dispersion compensation over E to L wavelength bands [11], large effective area [12], improved optical characteristics [13], high birefringence [14]. Square lattices were also studied [15] and a single-mode regime was presented [16] as well as large solid-cores [17, 18] and possibility of dispersion control [19]. Comparisons of different types of these lattices can be found for triangular

and square lattices [20], hexagonal and square lattices [21], and square, circular and hexagonal lattices [22].

Most of the publications cited above use gas infiltrating into the air-holes. However, in such a case, the control of characteristic quantities is difficult because its zero dispersion wavelength range is quite narrow. To overcome the mentioned limitations, recently a number of publications have been published, focused on infiltrating liquids into lattices in the photonic cladding or into cores of PCFs [23]. Selected aspects of such fibers have been analyzed, such as dispersion engineering [24], temperature sensitivity [25], influence of temperature on dispersion properties [26], infiltration with water [27], selective liquid-infiltration [28]. Liquid-infiltrated PCFs allowed for applications in fiber optic technology, e.g., in sensing [29] and supercontinuum generation [30, 31].

Most publications on liquid-infiltrated PCFs consider only hexagonal lattices. In this paper, we propose three solid-core PCF structures based on silica, with hexagonal, circular and square lattices, composed of 8 rings of air-holes surrounding the core, infiltrated with ethanol. The dispersion characteristics of these fibers were analyzed numerically. As a result, the optimal geometrical parameters set was determined to be used in applications in fiber optic technology.

In our work, the Lumerical Mode Solutions software was used [32] to design three solid-core PCFs with different types of lattice in the claddings, namely hexagonal, square and circular. Each structure has the same silica glass (SiO_2) as the base material. The lattices consist of 8 rings of air-holes surrounding the core, infiltrated with ethanol as shown in Fig. 1, where d is the air-hole diameter and Λ is the lattice constant.

In our simulations we used $\Lambda = 5 \mu\text{m}$, which allows to achieve an effective mode area comparable to the mode area of standard single-mode step-index fibers. The diameter of air-holes was set to 1.0 μm , 2.0 μm , 3.0 μm , and 4.0 μm [26]. To ensure fabrication feasibility and minimize loss in photonic crystal fibers, we have chosen

* E-mail: chuvanlanh@vinhuni.edu.vn

structures that consist of 8 rings of air-holes [33]. The fiber structures investigated are single-mode and multimode fibers. Structures with the filling factor $f = d / \Lambda < 0.4$ will yield single-mode fibers [4]. In the single-mode fibers, the light is very well confined in the core with a low loss. Consequently, they are capable of supercontinuum generation. In our study, only the dispersion characteristics of the fundamental modes are considered.

The real parts of the refractive index of ethanol and fused silica are shown in Fig. 2.

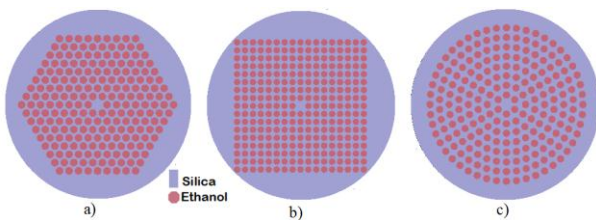


Fig. 1. The geometrical structure of the solid-core PCFs with (a) hexagonal, (b) square, and (c) circular lattices in the cladding, infiltrated with ethanol.

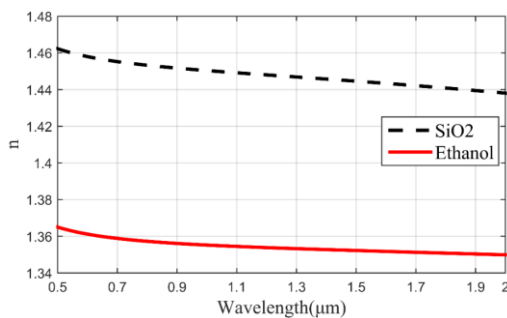


Fig. 2. Real part of the refractive index of ethanol [34, 35, 37] and fused silica [38].

Figure 3 shows the dispersion characteristics of the modeled PCFs. The shape of the dispersion characteristics for all three structures infiltrated with ethanol are similar. The steepest slope is in the wavelength range $0.5 \div 0.9 \mu\text{m}$. The dispersion characteristics are flat in the approximate range $0.9 \div 1.6 \mu\text{m}$. The most flat dispersion characteristics are located near the zero dispersion wavelength for $d = 1.0 \mu\text{m}$. This result agrees with the results published in the papers [25, 26, 39].

The highest dispersion is achieved for circular lattices while the smallest for hexagonal lattices, for a given wavelength and diameter of air-holes. In Table 1 the dispersion values for three PCF structures are shown, for a wavelength of $1.55 \mu\text{m}$. For $d = 1.0 \mu\text{m}$, the smallest dispersion is for the hexagonal lattice (22.2 ps/nm/km). The highest dispersion is for the circular lattice (23.1 ps/nm/km). For $d = 4.0 \mu\text{m}$, the smallest dispersion is for the hexagonal lattice (43.7 ps/nm/km) and the highest dispersion is for the circular lattice (45.4 ps/nm/km). As a result, for the hexagonal lattice, the dispersion

characteristics are flat and smaller than for the square and circular lattices. In effect, most works choose a hexagonal lattice for PCFs used for supercontinuum generation [10, 30, 31].

The analyzed PCFs have a zero dispersion wavelength (ZDW) in the near-infrared range as shown in Table 2. The ZDW is the biggest for hexagonal lattices and the smallest for circular lattices. Moreover, by increasing the diameter of air-holes, the ZDW of three PCFs decreases. The same phenomenon was observed in a PCF infiltrated with water [26]. When the diameter of air-holes is $1.0 \mu\text{m}$, the biggest ZDWs for hexagonal, square, circle lattices are $1.235 \mu\text{m}$, $1.224 \mu\text{m}$, and $1.191 \mu\text{m}$, respectively. These values are reduced to $1.066 \mu\text{m}$, $1.058 \mu\text{m}$, and $1.043 \mu\text{m}$, respectively, for the diameter of air-holes equal to $4.0 \mu\text{m}$. Thus, for the hexagonal lattice, the ZDW shift is 169 nm when the diameter of air-holes changes from $1 \mu\text{m}$ to $4 \mu\text{m}$. The shift equals 166 nm and 148 nm for square and circular lattices, respectively.

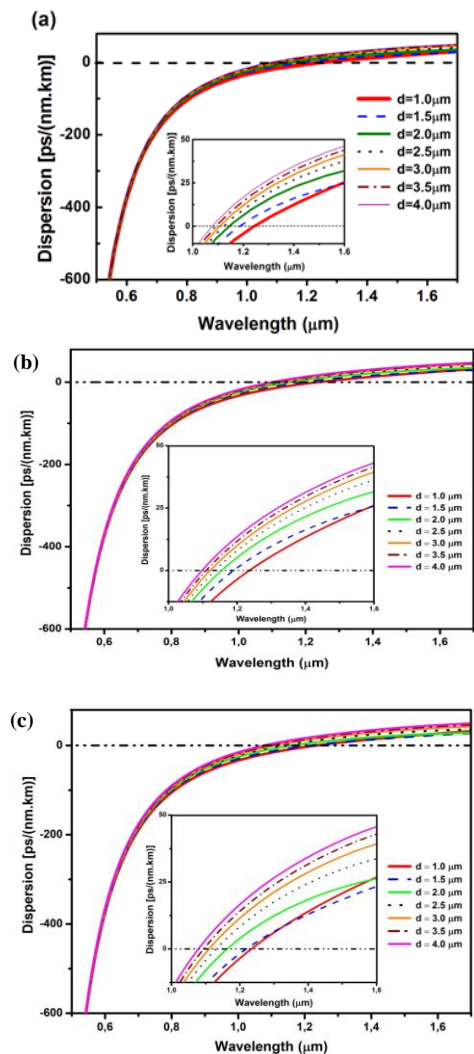


Fig. 3. Chromatic dispersion as a function of wavelength for the analyzed PCFs with various air-hole diameters infiltrated with ethanol: a) hexagonal, b) square, and c) circular lattice.

Table 1. Chromatic dispersion of the PCFs with various air-hole diameters, at 1.55 μm wavelength, infiltrated with ethanol, for a) hexagonal, b) square, and c) circular lattices.

λ (μm)	d (μm)	D (ps.(nm.km) ⁻¹)		
		Hexagonal	Square	Circle
1.55	1.0	22.2	22.9	23.1
	1.5	22.8	24.1	25.3
	2.0	30.0	31.8	32.6
	2.5	35.2	37.1	38.3
	3.0	38.8	39.9	41.2
	3.5	41.4	42.9	43.7
	4.0	43.7	44.5	45.4

Table 2. ZDWs for the PCFs with various air-hole diameters, infiltrated with ethanol for a) hexagonal, b) square, and c) circular lattices.

d (μm)	ZDW (μm)		
	Hexagonal	Square	Circle
1.0	1.235	1.224	1.191
1.5	1.196	1.187	1.165
2.0	1.136	1.124	1.112
2.5	1.127	1.119	1.100
3.0	1.096	1.076	1.057
3.5	1.073	1.067	1.048
4.0	1.066	1.058	1.043

In conclusion, the dispersion characteristics of solid-core photonic crystal fibers with different types of photonic lattice in the claddings, infiltrated with ethanol, have been simulated numerically and analyzed. The results show that the dispersion characteristics of the hexagonal lattice are flat and smaller than for the square and circular lattices. When the diameter of air-holes varies from 1 μm to 4 μm , ZDW for the hexagonal lattice shifted more than for the square and circular lattices and, thus it can be applied for supercontinuum generation.

This research is funded by Vietnam National Foundation for Science and Technology Development (NAFOSTED) under grant number 103.03-2020.03.

References

- [1] J.C. Knight, T.A. Birks, P.S.J. Russell, D.M. Atkin, *Opt. Lett.* **21**, 1547 (1996).
- [2] T.A. Birks, J.C. Knight, P.S.J. Russell, *Opt. Lett.* **22**, 961 (1997).
- [3] J.B. Jensen *et al.*, *IEEE Sensors* **1**, 1562 (2003).
- [4] R. Buczyński, *Acta Phys. Polon. A* **106**, 141 (2004).
- [5] S. Li, X. Zhang, G.P. Agrawal, *Appl. Opt.* **52**, 3088 (2013).
- [6] A. Ghunawat *et al.*, *Opt. Wireless Technol.* **105**, 265 (2018).
- [7] T. Baghdasaryan *et al.*, *Opt. Expr.* **19**, 7705 (2011).
- [8] R. Buczynski *et al.*, *Opto-Electr. Rev.* **20**, 207 (2012).
- [9] Y.E. Monfared *et al.* *Optik* **124**, 7049 (2013).
- [10] M. Klimczak *et al.* *Opt. Lett.* **38**, 4679 (2013).
- [11] M.M. Haque *et al.*, *J. Microwaves Optoelectr.* **12**, **44** (2013).
- [12] G. Prabhakar *et al.*, *Appl Opt.* **52**, 4505 (2013).
- [13] S. Geerthana *et al.*, *J. Nonlin. Opt. Phys. Mat.* **24**, 1550051 (2015).
- [14] M. Karthika, S. Selvendran, K. Saravanan, *Internat. J. Pure and Appl. Mat.* **118**, 1 (2018).
- [15] A.H. Bouk *et al.*, *Opt. Exp.* **12**, 941 (2004).
- [16] E. Poli *et al.*, *J. Opt. Soc. Am. A* **22**, 1655 (2005).
- [17] H. Demir, S. Ozsoy, *Opt. Fiber Technol.* **17**, 594 (2011).
- [18] H.D. Inci, S. Ozsoy, *Opt. Mat.* **35**, 205 (2012).
- [19] J. Park, S. Lee, S. Lee, S.E. Kim, K. Oh, *Opt. Expr.* **20**, 5281 (2012).
- [20] M.O. Faruk *et al.*, *WCECS 2*, San Francisco, USA (2010).
- [21] B. Dabas, R.K. Sinha, *Opt. Commun.* **283**, 1331 (2010).
- [22] M. B. Hossain *et al.*, *Opt. Photon. J.* **7**, 235 (2017).
- [23] A. Lorenz *et al.*, *Opt. Expr.* **18**, 3519 (2010).
- [24] J. Pniewski *et al.*, *Appl. Opt.* **55**, 5033 (2016).
- [25] C.V. Lanh *et al.*, *Proc. SPIE* **9816**, 981600 (2015).
- [26] D.X. Khoa, C.V. Lanh, C.L. Van, H.D. Quang, M.V. Luu, M. Trippenbach, R. Buczyński, *Opt. Quantum Electr.* **49**, 1 (2017).
- [27] D.X. Khoa, C.V. Lanh, H.D. Quang, M.V. Luu Van, M. Trippenbach, R. Buczynski, *Appl. Opt.* **56**, 1012 (2017).
- [28] H. Liu *et al.*, *Photon. Sensors* **9**, 213 (2019).
- [29] M.F.H. Arif, M.J.H. Biddut, *Sens. Bio-Sens. Res.* **12**, 8 (2017).
- [30] C.V. Lanh *et al.*, *J. Opt.* **19**, 125604 (2017).
- [31] C.V. Lanh *et al.*, *Laser Phys.* **29**, 5107 (2019).
- [32] Lumerical Solutions, <http://www.lumerical.com/tcad-products/mode/>
- [33] V. Finazzi *et al.*, *IEEE Photon. Technol. Lett.* **15**, 1246 (2003).
- [34] S. Kedenburg, M. Vieweg, T. Gissibl, H. Giessen, *Opt. Mater. Expr.* **2**, 1588 (2012).
- [35] R. Wang *et al.*, *Sensors* **13**, 7916 (2013).
- [36] K. Nielsen *et al.*, *J. Opt. A: Pure Appl. Opt.* **7**, L13 (2005).
- [37] K. Moutzouris *et al.*, *Appl. Phys. B.* **116**, 617 (2014).
- [38] I.H. Malitson, *J. Opt. Soc. Am.* **55**, 1205 (1965).
- [39] L.V. Hieu, C.L. Van, N.T. Hue, N.M. An, R. Buczyński, R. Kasztelanica, *Laser Physics* **28**, 115106 (2018).